Performance Evaluation and Optimal Design of Supermarket Refrigeration Systems with Supermarket Model “SuperSim”, Part II: Model Applications

Y.T. Ge*, S.A. Tassou

Mechanical Engineering, School of Engineering and Design, Brunel University,

Uxbridge, Middlesex, UB8 3PH, UK

ABSTRACT

As described in Part I, the supermarket simulation software “SuperSim” with its integrated refrigeration, building and HVAC system models, can be used to evaluate, compare and optimize alternative supermarket refrigeration systems. In Part II the model was used to evaluate and compare the performance of a CO_2 booster refrigeration system with that of a conventional R404A multiplex system in a supermarket application. Floating head pressure control was implemented for both systems when they are in subcritical cycles. For the CO_2 system, when the system was in transcritical cycle due to higher ambient air temperature, the head pressure was optimized through extensive thermodynamic cycle analysis as a function of ambient air temperature. The performance of the CO_2 booster system in the supermarket was then simulated during a one-year period and compared with that of R404A system. As a result, the system performance will benefit from a lower ambient temperature and a sizeable heat recovery for the CO_2 system.

Key Words: supermarket, model, CO_2 , R404A, control, comparison.

* Corresponding author. Tel.:+44 1895 266722; fax: +44 1895 256392.
E-mail address:yunting.ge@brunel.ac.uk

NOMENCLATURE

c_1-c_6	coefficients
DT	temperature difference (K)
h	enthalpy (J kg^{-1})
P	pressure (Pa or bar)
Q	capacity , heat load (kW)
R	ratio
Tamb	ambient air temperature (°C)
t,T	temperature (°C)
TT	transition temperature (°C)
W	power (kW)
x	quality
y	mass flow rate ratio

Greek symbol

η	efficiency

Subscripts

amb	ambient
cd,min	minimum condensing

cp	compressor
ev	evaporator
fan	condenser fan
H	high side
is	isentropic
P	pressure
ss	saturated suction
vent	ventilation

1. Introduction

Alongside the other application areas such as heat pumps and automotive air conditioning, CO_2 refrigerant has attracted significant attention for application to supermarket refrigeration systems. The energy consumption of a typical supermarket in the UK is within the region of 1000 kWh/m^2, of which 30% to 50% is used for refrigeration (Tassou, 2007). This substantial consumption of energy in the form of grid electricity and gas makes a significant contribution to indirect CO_2 emissions. HFC refrigerants such as R404A, which are currently used in modern supermarket refrigeration systems, also contribute significantly to direct CO_2 emissions. In contrast to the aforementioned HFC refrigerants, CO_2 refrigerant is more environmentally friendly, due to its zero Ozone-Depletion Potential (ODP) and negligible direct Global Warming Potential (GWP<1). It also has favourable thermophysical properties which include higher density, latent heat, specific heat, thermal conductivity and volumetric cooling capacity, and lower viscosity than HFC refrigerants that lead to better heat transfer. The application of CO_2 refrigerant to supermarket refrigeration systems can almost entirely eliminate direct CO_2 emissions and has even the potential to reduce indirect emissions. However, CO_2 has a relatively high operating pressure and low critical temperature, such that an air cooled CO_2 system will not be able to condense the refrigerant in the condenser during periods of high ambient temperatures. The higher pressure and transcritical operation during periods of high ambient temperatures can lead to higher energy consumption for CO_2 systems compared to R404A when they are designed on the principle of the basic single stage vapour compression cycle and used for chilled food applications with evaporating temperatures down to around -10.0 ^{o}C (Sarkar et al., 2005**)** The efficiency of CO_2 systems can be improved through the implementation of more sophisticated cycles and advanced control techniques.

In general, three types of CO_2 system designs have been applied in supermarket refrigeration applications(Sawalha, 2008): indirect systems (Hinde et al.,2009) , cascade systems (Eggen and Aflek , 1998) and all CO_2 transcritical systems (Nekså and Girotto, 2002; Schiesaro and Kruse , 2002). For the indirect system application, the CO_2 fluid is used as a two-phase secondary coolant which has shown some advantages over conventional single-phase fluids, such as lower pumping power, smaller pipe sizes and excellent heat transfer properties. On the primary side, however, a HFC refrigerant such as R404A or R507C is still commonly used. For a cascade system, a fluid such as R404A, R134a, NH_3, a hydrocarbon, or even CO_2 can be employed in the higher cascade for heat rejection, and CO_2 operates in a subcritical cycle in the lower cascade. The cascade CO_2 system has several advantages, including reduced low-temperature compressor sizes, the absence of a liquid pump and fewer stages of heat transfer compared to indirect or 'booster' systems (Kim et al., 2004). It has also been reported that the energy consumption of the cascade system can be either neutral or less than that of conventional R404A systems (Christensen and Bertilsen, 2003). However, many indirect and cascade CO_2 systems tend to use HFC refrigerants in the primary side, which will not facilitate to entirely eliminate any direct environmental impact.

For an all CO_2 booster system, advantages reported include simpler and cheaper system designs with one fluid and one circuit (at medium temperatures and low temperatures) and heat recovery potential although the utility was found significantly low during winter period (Arias and Lundqvist, 2006). It has been discovered, however, that the total annual energy consumption of an all CO_2 system in a hot climate can be higher than that of a conventional R404A system (Girotto et al., 2003, 2004). Systems installed in Northern European countries such as Sweden, Denmark, Germany and Switzerland, in contrast, can have an equivalent or lower annual energy consumption than R404A systems, due to the higher number of hours during the year in which such systems operate in the subcritical mode (Girotto et al., 2004).

In this paper, an all CO_2 booster system is considered and its performance compared with that of an R404A system in a supermarket application in the North of England using the SuperSim model. For both systems optimum head pressure control is implemented with respect to ambient temperature.

2. CO_2 booster refrigeration system

2.1 System layout

A schematic of a typical CO_2 booster system used in supermarket refrigeration applications is shown in Fig. 1. The booster cycle has four pressure regions, high, intermediate, medium and low. The high pressure region extends from the outlet of the high stage compressor (COMP_HI) through to the gas cooler or condenser, depending on ambient conditions, the suction line heat exchanger (SHX), and to the high pressure control valve (CV_HP). The intermediate pressure region begins at the outlet of the CV_HP and extends through the receiver (REC) to the expansion valves of the medium (EV_MT) and low temperature (EV_LT) evaporator coils. The medium pressure region begins at the outlet of the medium temperature (MT) expansion valve and extends through the evaporator coils of the medium temperature cabinets and chilled food cold rooms of the supermarket. The low pressure region starts at the outlet of the (LT) expansion valve and extends through the evaporator coils of the frozen food display cabinets and cold rooms up to the low stage compressors (COMP_LO). The refrigerant from the LT compressors mixes with the refrigerant from the MT evaporator coils and the mixture then further mixes with the expanded vapour from the receiver through the bypass valve (BPV_1). The mixture then flows through the superheating heat exchanger, SHX, before entering the high stage compressors ,COMP_HI. In this system, a second bypass valve (BPV_2) is included to bypass the SHX in the event the 'hot' side fluid temperature from the gas cooler/condenser is lower than 'cold' side fluid temperature at '14'. This situation may occur at low ambient temperatures when the system operates in the subcritical region.

2.2 Optimal high side pressure of transcritical cycle

When the high side pressure is above the critical value due to high ambient temperature, the system will operate in the transcritical region as shown in the corresponding P-h diagram in Fig. 2. To simplify the analysis, the refrigerant states at the outlet of the MT and LT evaporators are both assumed to be saturated vapour. For such a system, which is similar to a single stage CO_2 transcritical cycle, it is expected that an optimal high side pressure exists that maximises the COP for each ambient temperature (Ge and Tassou, 2009; Liao et al., 2000; Chen and Gu,2005; Cecchinato et al., 2009). The optimum pressure for each ambient temperature can be determined through cycle analysis as follows:

If the ratio of refrigerant mass flow rate through the MT evaporator coils to the total flow rate through the MT and LT coils is *y* and the refrigerant quality at the outlet of CV_HP is *x*, the cooling COP of the system can be calculated as:

$$COP = \frac{y(1-x)(h_9-h_8)+(1-y)(1-x)(h_{11}-h_{10})}{(h_1-h_{15})+(1-y)(1-x)(h_{12}-h_{11})} \quad (1)$$

Mathematically, the optimal high side pressure P_H can be obtained by solving the following differential equation:

$$\frac{\partial \boldsymbol{COP}}{\partial \boldsymbol{P_H}} = \mathbf{0} \quad (2)$$

To solve equation (2), equation (1) is rearranged as:

$$COP = \frac{y(h_9-h_8)+(1-y)(h_{11}-h_{10})}{\left(\frac{h_1-h_{15}}{1-x}\right)+(1-y)(h_{12}-h_{11})} \quad (3)$$

Let ,

$$F_1 = y(h_9-h_8)+(1-y)(h_{11}-h_{10}) \quad (4)$$

and,

$$F_2 = (1-y)(h_{12}-h_{11}) \quad (5)$$

then,

$$COP = \frac{F_1}{\left(\frac{h_1-h_{15}}{1-x}\right)+F_2} \quad (6)$$

Differentiating equation (2) gives:

$$\frac{\partial COP}{\partial P_H} = \frac{\frac{\partial F_1}{\partial P_H}\left[\left(\frac{h_1-h_{15}}{1-x}\right)+F_2\right]-F_1\left[\frac{\partial\left(\frac{h_1-h_{15}}{1-x}\right)}{\partial P_H}+\frac{\partial F_2}{\partial P_H}\right]}{\left[\left(\frac{h_1-h_{15}}{1-x}\right)+F_2\right]^2} = 0 \quad (7)$$

Since both F_1 and F_2 are independent of P_H, $\frac{\partial F_1}{\partial P_H}$ and $\frac{\partial F_2}{\partial P_H}$ are both equal to zero.

Therefore equation (7) can be simplified as:

$$\frac{\partial\left(\frac{h_1-h_{15}}{1-x}\right)}{\partial P_H}=0 \quad (8)$$

Rearranging gives:

$$(1-x)\left[\frac{\partial h_1}{\partial P_H}-\frac{\partial h_{15}}{\partial P_H}\right]+(h_1-h_{15})\frac{\partial x}{\partial P_H}=0 \quad (9)$$

Equation 9 indicates that the optimum high side pressure is independent of the refrigerant mass flow ratio y. The equation is highly non-linear and difficult to solve mathematically although iteration solving method can be utilized (Srinivasan et al. , 2010). Therefore sensitivity analysis was applied to identify the parameters that could maximize COP as a function of gas cooler pressure. After extensive simulations, it was identified that the optimal high side pressure is mainly dependent on compressor performance characteristics, the effectiveness of the SHX and the ambient air temperature. If the effectiveness of the SHX is assumed to be constant, for given compressor characteristics the optimal high side pressure is only a function of ambient air temperature. For the booster system considered in this paper, a number of Bitzer CO_2 semi-hermetic reciprocating compressors, with the same type of 4FTC-20K were chosen for the high pressure stage, COMP_HI, and some semi-hermetic compressors with type of 2EHC-3K for the low pressure stage, COMP_LO, of the system. The isentropic efficiency of each above compressor type is a function of the pressure ratio as follows:

For the transcritical compressor:

$$\eta_{is}=0.7595-0.0328R_p \quad (10)$$

and for the subcritical compressor:

$$\eta_{is} = 0.7178 - 0.038 R_p \quad (11)$$

The refrigerant mass flow rate ratio y was set to 0.8 to satisfy the design refrigeration loads at each temperature level, MT and LT. The intermediate pressure was set at 30 bar and the effectiveness of the SHX was assumed to be 0.8. The variation of the system COP for a range of ambient temperatures between 25°C and 40°C was predicted with the simulation model and the results are shown in Fig. 3. It can be seen that for each ambient temperature there is a high stage pressure that maximises the COP and this optimum pressure increases as the ambient temperature increases. For ambient temperatures above 27 ^{o}C, the relationship between ambient temperature and optimum high side pressure is almost linear and this is shown in Fig. 4.

2.3 Overall control strategies of high side refrigerant pressure

During one year operational period when ambient air temperature is low, the CO_2 system will be in all subcritical cycles and the corresponding control strategy for the high side pressure need also to be designed correspondingly. One ambient air temperature, 21°C, with ±1°C deadband is used to signify the transition point for subcritical and transcritical cycles **(**Ge and Tassou, 2009). When the system is in all subcritical cycles, floating head pressure control strategy is utilized with temperature differences of 10 K and the minimum condensing temperature is set to 10°C. It should note that the transition temperature can be increased supposing the temperature difference is less than 10 K due to higher efficient or larger size of condensers are utilized. In general, the control strategy of high side pressure for the supermarket CO_2 booster refrigeration system is quantified as below:

When TAT=21±1°C,

$$P_H\,(bar) = \begin{cases} 44.97 & \text{when } t_{amb} < 0°C \\ 1.352t_{amb} + 44.34 & \text{when } 0\,°C \le t_{amb} \le 20\,°C \\ 72.05 & \text{when } 20°C < t_{amb} < 22°C \text{ and subcritical cycle is on} \\ 75 & \text{when } 20°C < t_{amb} < 22°C \text{ and transcritical cycle is on} \\ 75 & \text{when } 22°C \le t_{amb} \le 27°C \\ 2.3426t_{amb} + 11.541 & \text{when } t_{amb} > 27°C \end{cases} \quad (12)$$

2.4 Compressor selections

In the simulation, semi-hermetic reciprocating compressors from a refrigeration compressor manufacturer were selected for the CO_2 and R404A refrigeration systems. The number of compressors on each compressor pack was based on the load in Part I of the paper. The coefficients $c_1 \sim c_6$ for the compressor model described in Part I were determined from manufacturer performance characteristics and are listed in Table 1.

3. Model prediction

3.1 Operating states

The control strategies and compressor specifications described above for the CO_2 booster system were integrated into the validated supermarket refrigeration model demonstrated in Part I so as to investigate and compare the performance of the CO_2 system with that of a conventional R404A system. The supermarket details illustrated in Part I including weather data, building construction, HVAC layout and refrigeration load were used in the modelling of the two refrigeration systems, R404A multi-compressor system and CO_2 booster system. For the R404A system, floating head pressure control was employed and heat recovery from the system was not considered. Heat recovery was considered for the CO2 system for both transcritical and subcritical operation. The control parameters employed for the two systems are detailed in Table 2.

For the R404A system, floating head control was used with temperature differences between condensing and ambient temperatures of 15 K and 10 K for the MT and LT temperature packs respectively, while the minimum condensing temperature for each pack was fixed at 20°C and 10°C respectively. For the purpose of comparison, the evaporating temperatures of the MT and LT packs for both refrigerants were controlled at -10°C and -32°C respectively although these values can be increased when higher efficient or larger size of evaporators are utilised. For the CO_2 system, the control strategies detailed by equation (12) were employed. For comparison purposes the same evaporating temperatures as the R404A system were used for the MT and LT evaporators.

Fig. 5 shows the variation of the high side pressures with ambient air temperature for the R404A and CO_2 refrigeration systems during a year. To make it clearer, for the R404A system, only the pressure of MT pack is shown in the diagram. The pressure variation for the LT pack is similar to that of MT but with relatively lower value. It can be seen that the variation of the high side pressures follow to a large extent the variation of the ambient temperature as the systems use floating head pressure control. Only at low ambient temperatures below 5°C for the MT R404A pack and 0°C for LT pack (not shown), the high side pressures remain fairly constant as the packs operate at minimum condensing pressures set by the control system.

Fig. 6 shows the variation of the high side pressures with ambient temperature for a summer day for the two systems.

. It can be seen that the high side pressures of the two systems remain fairly constant up to 11.00 a.m. in the morning when the ambient temperature is below 20 ^{o}C. When the temperature rises above 20 ^{o}C the high side pressure of the two systems increase with the increase in ambient temperature. The CO_2 system enters the transcritical region of operation with the head pressure controlled at the optimum value for each ambient temperature as shown in Fig. 4. The system drops into the subcritical operating region after approximately 8.0 p.m.

3.2 Performance comparison

The variation of the compressor power consumption of the R404A packs (MT pack and one LT pack) with ambient temperature for a summer and winter day is shown in Fig. 7.

It can be seen that the influence of ambient temperature on the power consumption of the LT packs is not as significant as that for the MT packs due to the lower impact of store conditions on the load of the LT refrigeration fixtures in the store. This is as a result of the lower infiltration load of LT fixtures due to the use of well and glass door cabinets for the display of frozen food products. In the summer, the power consumption of the MT pack almost doubles from around 60 kW to over 100 kW as the ambient temperature increases from around 17 ^{o}C to 32 ^{o}C.

Fig. 8 shows the variation of the power consumption of the low and high pressure stage of the CO_2 booster system for the summer day. It can be seen that the power consumption of the LT stage remains fairly constant because it is, to a large extent, isolated from the effect of variation of the ambient temperature. The main effect that the ambient conditions have is an indirect effect due to its influence on internal store conditions. The influence of the ambient temperature on the power consumption of the high pressure side compressors, however, can be significant. During operation at subcritical conditions the high stage power consumption does not change significantly with ambient temperature. As the system enters the transcritical region, however, the power consumption of the high stage compressors rises rapidly to over 160 kW.

The variation of power consumption with ambient temperature of the two compressor stages for a winter day is shown in Fig. 9. As with a summer day it can be seen that the power consumption of the low stage compressors remain fairly constant whereas the power consumption of the high stage compressors increases significantly during the day when the ambient temperature rises. This is the reason that for high stage compressors when ambient air temperature increases both compression ratio and system cooling load will increase, which can contribute notably the power consumption of compressors.

Fig. 10 shows the variation of the COP of the R404A and CO_2 refrigeration systems as a function of ambient temperature. The COP of each system was calculated based on the total refrigeration load of the supermarket, low temperature plus medium temperature, divided by the power consumption of the refrigeration plant to deliver this refrigeration load. It can be seen that at low ambient temperatures, below about 10 ^{o}C, the transcritical CO_2 booster system offers a higher COP than the R404A system which increases as the ambient temperature decreases. Above 10 ^{o}C the COP of the R404A system becomes higher than that of the CO_2 system. The better performance of the CO_2 system at low temperatures is because that the system is in subcritical cycles and the compression ratio is largely reduced.

The heat recovery potential is dependent on the control strategies of both high side pressure of refrigerants and the HVAC system described in Part I. By comparing the ambient air temperature and controlled space temperature of the sales area, the outdoor air requirements and inlet conditions to the heat reclaim coil (HRC) can be determined. Fig. 11 shows predictions of the heating load of the sales area of the supermarket and the heat recovery potential of the CO_2 refrigeration system. It can be seen that during the winter months heat recovery from the CO_2 system will be in the region of 30 kW whereas the space heating requirement will be around 150 kW. During summer period, the heating load is reduced but still exists due to higher cooling infiltration load from the cabinet. In the meant time, heat recovery from the CO_2 system increases whereas the space heating load reduces to a point where heat recovery can satisfy all the space heating requirements of the supermarket.

Table 3 shows a comparison of the energy performance of the CO_2 booster system and a conventional R404A system in the supermarket. The simulations assumed that no heat recovery from the R404A plant due to the implementation of floating head pressure control. It can be seen that the energy consumption of the compressor packs for the two systems is fairly similar with the CO_2 booster system shown a 2.3% higher energy consumption than the R404A system. An advantage of the CO2 system is its energy recovery potential and the simulations show that for the supermarket studied, heat recovery can provide 40% energy savings in the space heating energy requirement compared to a R404A system with floating head pressure control and no heat recovery.

4. CONCLUSIONS

The supermarket model 'SuperSim' has been used to compare the performance of a conventional R404A refrigeration system and a CO_2 booster system. The controls of both systems were optimized to yield maximum seasonal efficiencies.

For weather conditions in the North of England the two refrigeration systems were found to lead to very similar energy consumption. Making maximum utilization of floating head pressure control, reduces significantly heat recovery opportunities from the R404A system. The booster CO_2 system, however, due to the higher cycle pressures and temperatures lends itself for heat recovery even during operation at subcritical conditions. For the supermarket investigated it was found that heat recovery can satisfy 40% of the space heating demand of the supermarket.

References

Arias J., Lundqvist P., 2006. Heat recovery and floating condensing in supermarkets. Energy and Buildings 38 ,73–81.

Cecchinato L., Chiarello M., Corradi M., Fornasieri E., Minetto S., Stringari P., Zilio C., 2009. Thermodynamic analysis of different two-stage transcritical carbon dioxide cycles. International Journal of Refrigeration 3 2 ,1 058 – 1067.

Chen Y., Gu J., 2005. The optimum high pressure for CO2 transcritical refrigeration systems with internal heat exchangers. International Journal of Refrigeration 28, 1238 – 1249.

Christensen K.G., Bertilsen P., 2003. Refrigeration systems in supermarket with propane and CO_2-energy consumption and economy. 21st IIR international congress of refrigeration, Washington, D.C., USA.

Eggen G., Aflek K.,1998. Commercial refrigeration with ammonia and CO_2 as working fluids, Natural Working Fluids ’98, IIR-Gustav Lorentzen Conference on Natural Working Fluids, Oslo, Norway, IIR, June 2-5.

Ge Y.T., Tassou S.A., 2009. Control optimisation of CO_2 cycles for medium temperature retail food refrigeration systems. International Journal of Refrigeration 3 2 , 1 3 7 6 – 1 3 8 8.

Girotto S., Minetto S., Nekså P.,2003. Commercial refrigeration system with CO_2 as refrigerant experimental results, 21st IIR international congress of refrigeration, Washington, D.C., USA.

Girotto S., Minetto S., Nekså P.,2004. Commercial refrigeration system using CO_2 as the refrigerant. International Journal of Refrigeration 27 ,717-723.

Hinde D., Zha S., Lan L.,2009. Carbon dioxide in north American supermarket, ASHRAE Journal, 18-24.

Kim M.H., Pettersen J., Bullard C.W., 2004. Fundamental process and system design issues in CO_2 vapor compression systems. Progress in Energy and Combustion Science 30, 119-174.

Liao S.M., Zhao T.S., 2000. Jacobsen A. A correlation of heat rejection pressures in transcritical carbon dioxide cycles. Applied Thermal Engineering 20, 831-841.

Nekså P., Girotto S., 2002. CO_2 as refrigerant within commercial refrigeration, therotical considerations and experimental results, 5th IIR-Gustav Lorentzen Conference on Natural Working Fluids, September 17-20, Guangzhou, China.

Sarkar J., Bhattacharyya S., Gopal MR, 2005. Transcritical CO2 heat pump systems: exergy analysis including heat transfer and fluid flow effects. Energy Conversion and Management 46, 2053–2067.

Sawalha S., 2008. Theoretical evaluation of trans-critical CO_2 systems in supermarket refrigeration, Part I: Modeling, simulation and optimization of two system solutions. International Journal of Refrigeration 31, 516-524.

Sawalha S., 2008. Theoretical evaluation of trans-critical CO_2 systems in supermarket refrigeration, Part II: System modifications and comparisons of different solutions. International Journal of Refrigeration 31, 525-534.

Schiesaro P., Kruse H., 2002. Development of a two stage CO_2 supermarket system, IIF-IIR, New technologies in commercial refrigeration, Urbana, Illinois, USA.

Srinivasan K., Sheahen P., Sarathy C.S.P., 2010. Optimum thermodynamic conditions for upper pressure limits of transcritical carbon dioxide refrigeration cycle, International Journal of Refrigeration 33, 1395-1401.

Tassou S.A., 2007. Potential for Solar Energy in Food Manufacturing, Distribution and Retail. Report to DEFRA, AC045, 25 pgs.

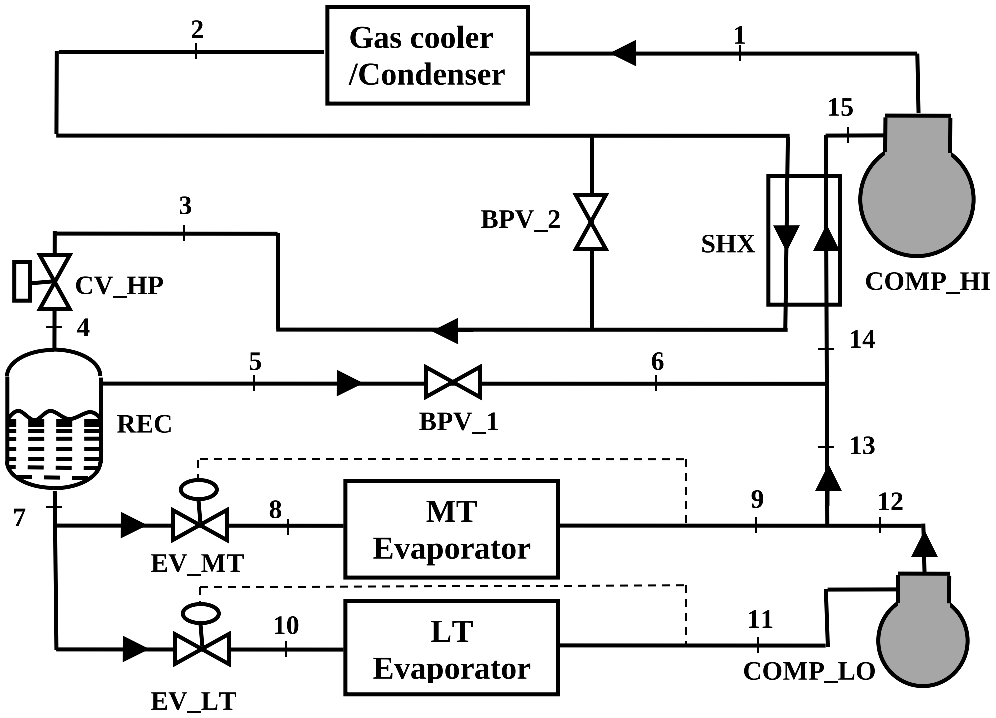

Fig. 1- A typical CO_2 booster system applied in supermarket refrigeration system

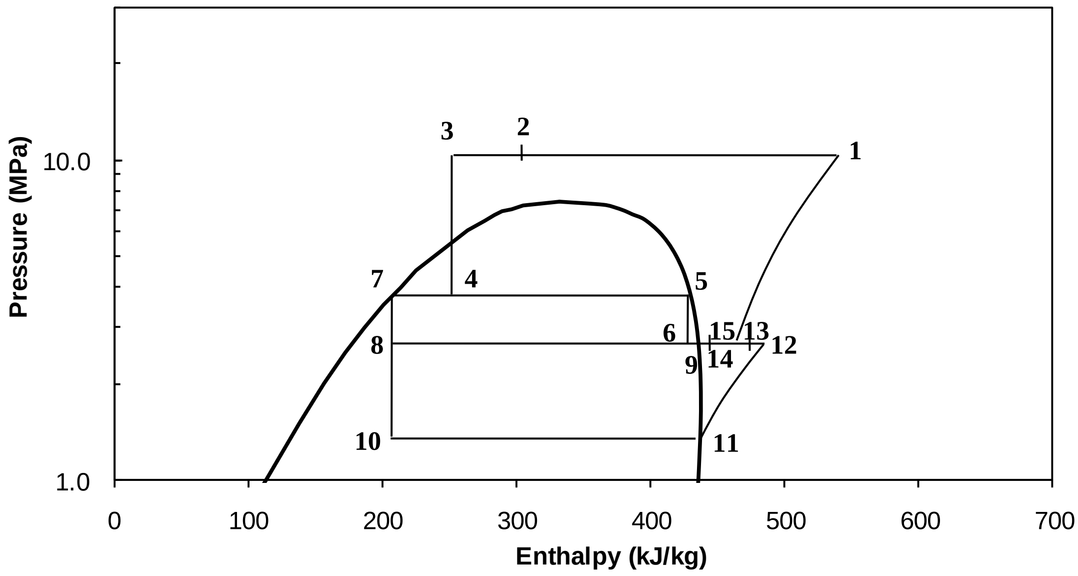

Fig. 2- P-h diagram of transcritical cycle in the CO2 booster system

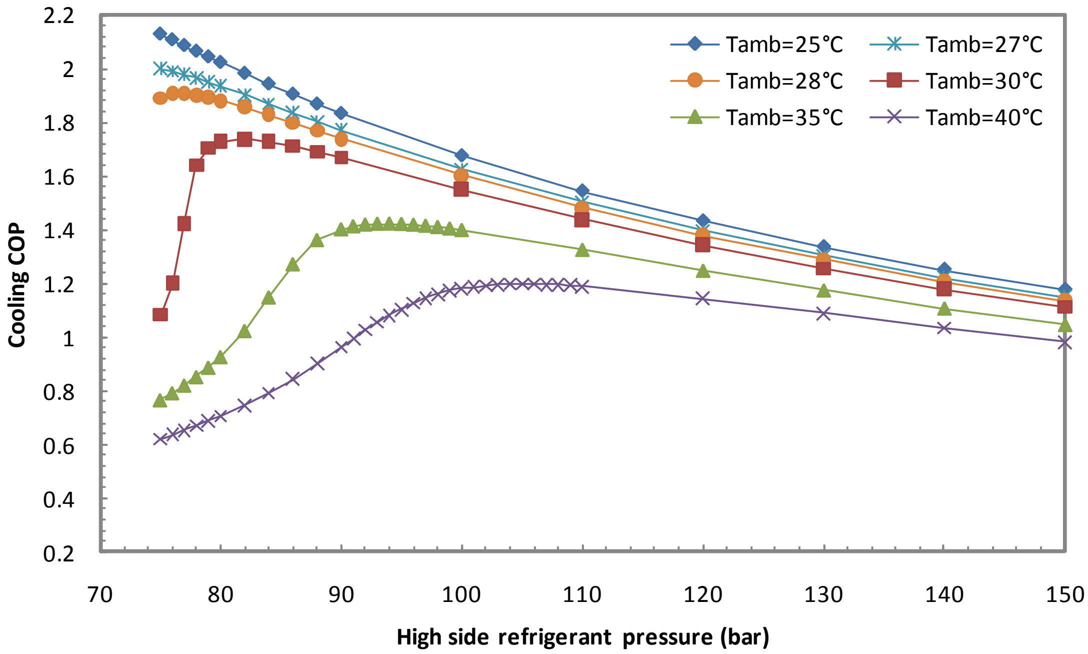

Fig. 3- Variation of COP with high side refrigerant pressure and ambient air temperature for the transcritical CO_2 booster system

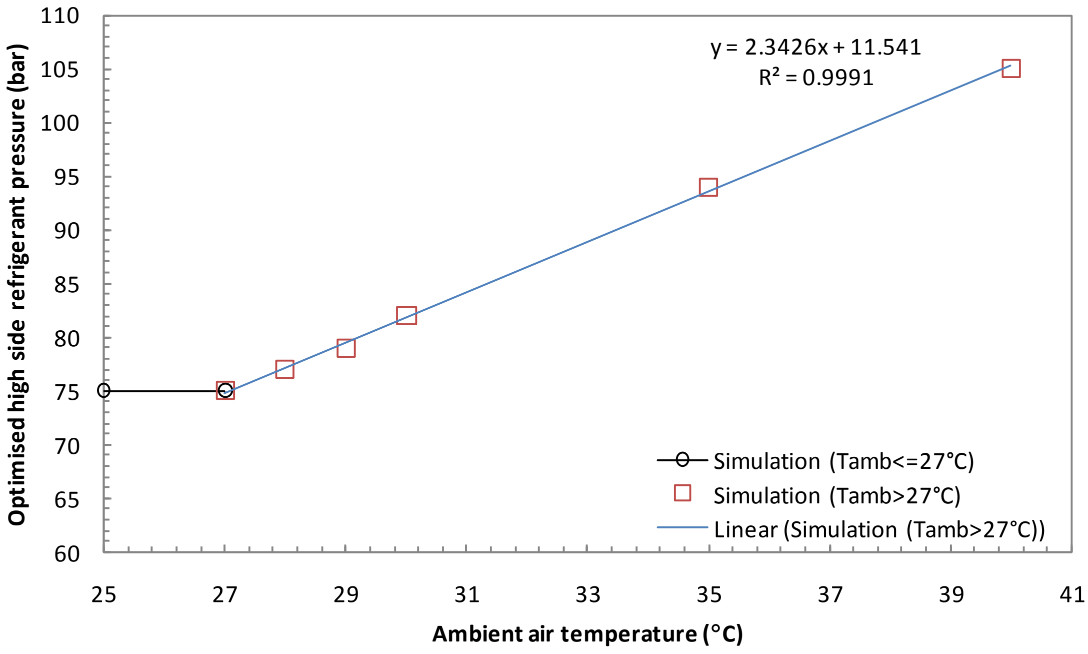

Fig. 4- Variation of optimised high side refrigerant pressure with ambient air temperature for the transcritical CO2 booster system

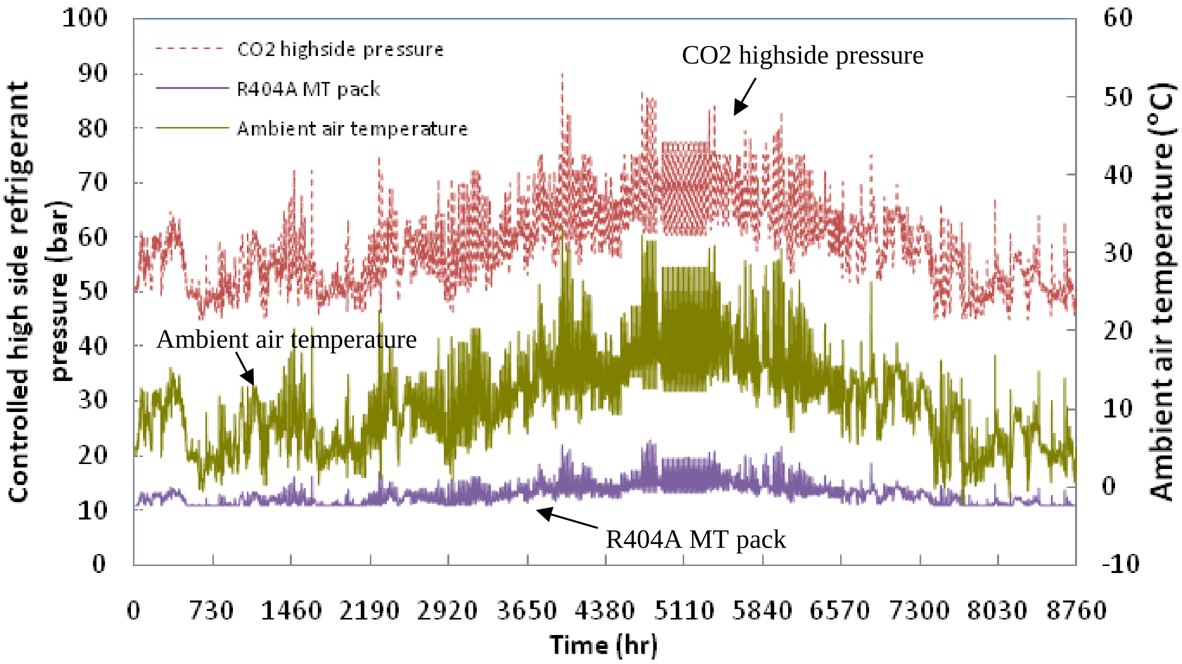

Fig. 5- Variation of ambient air temperature and high side pressures for different systems in Table 2.

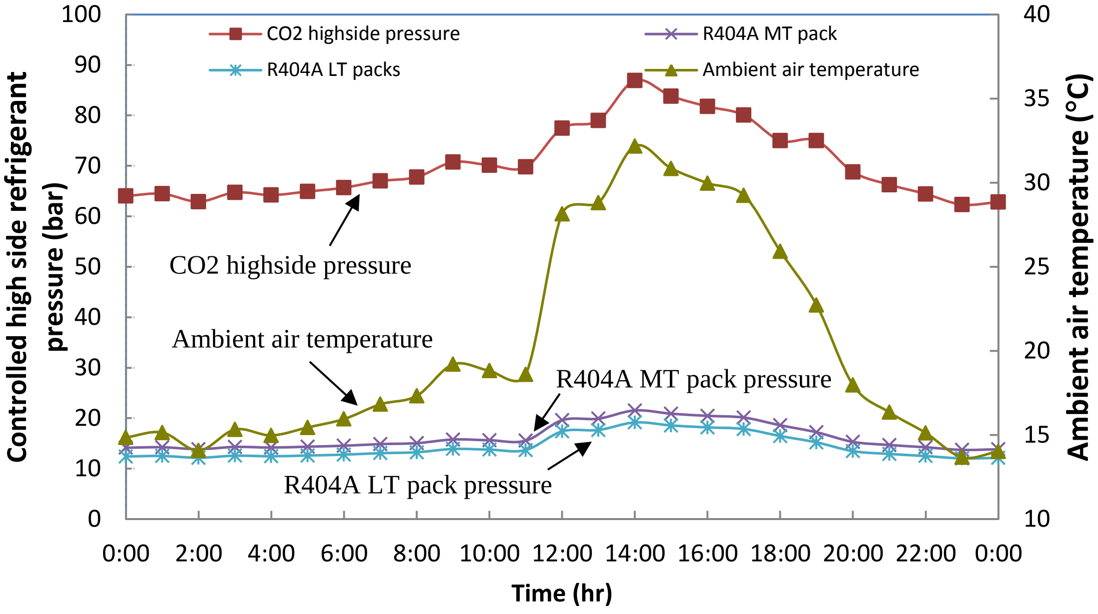

Fig. 6- Variation of ambient air temperature and high side pressures for a typical summer day

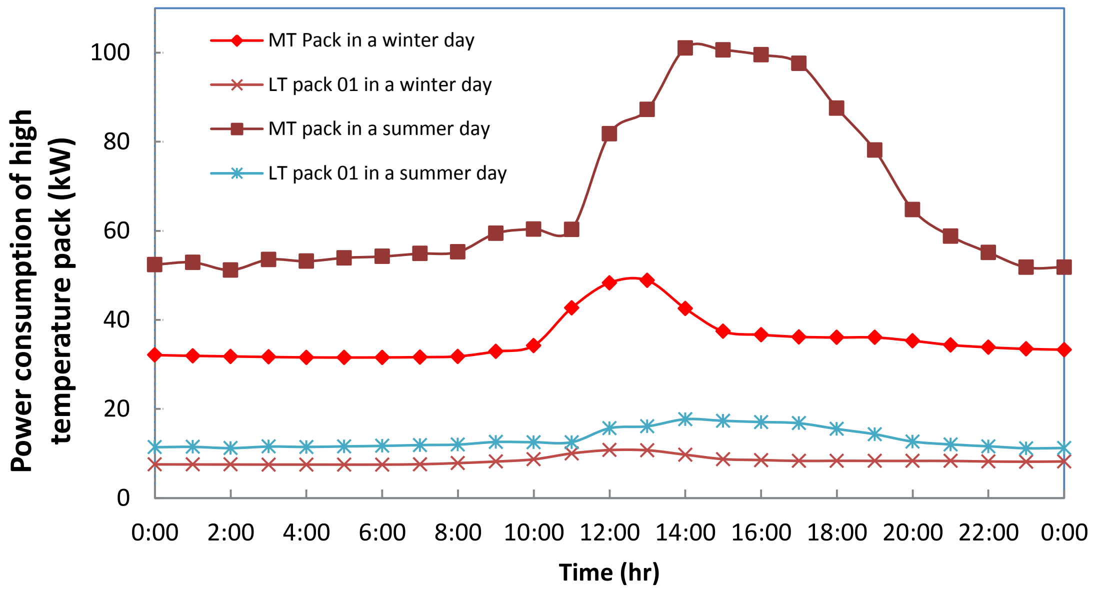

Fig. 7- Variation of compressor power consumption for the R404A packs for a summer and winter day.

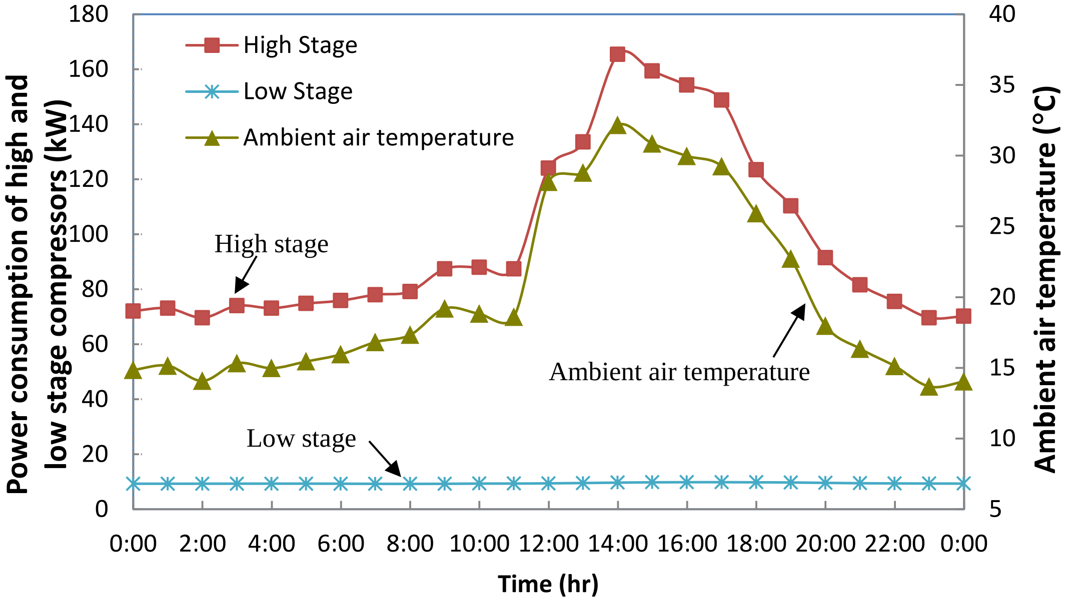

Fig. 8- Variations of compressor power consumptions for the CO_2 refrigeration system in a summer day.

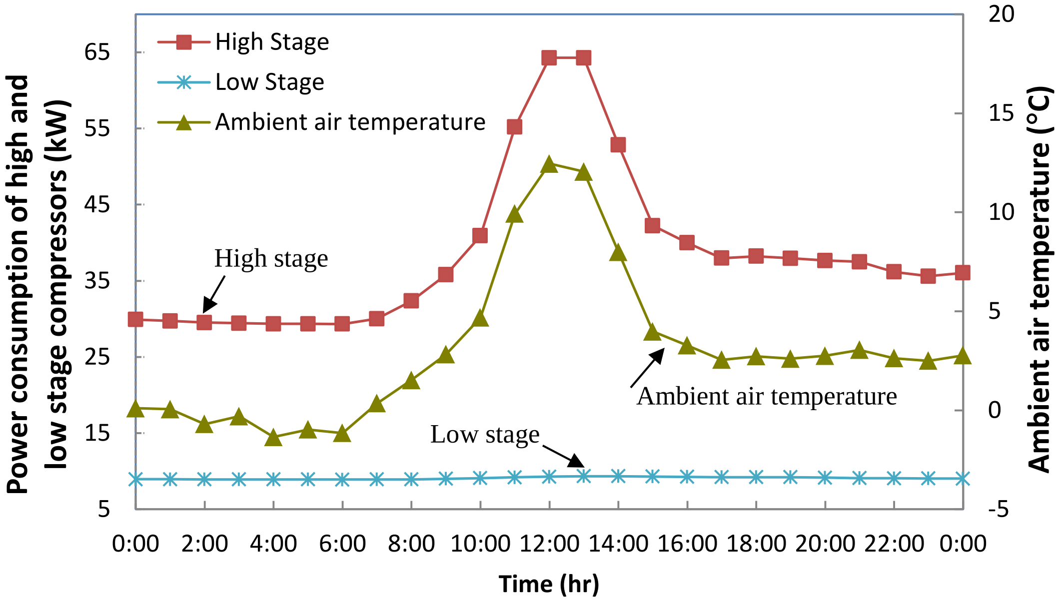

Fig. 9- Variation of ambient temperature and compressor power for the CO_2 refrigeration system in a winter day

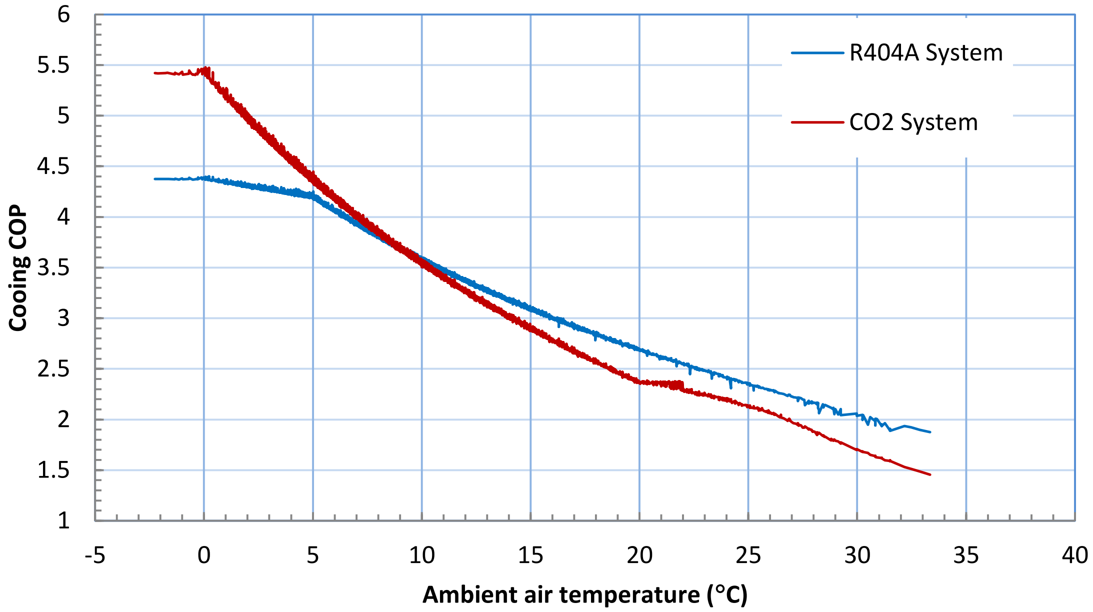

Fig. 10- Variation of cooling COP with ambient air temperature for R404A and CO_2 refrigeration systems.

;

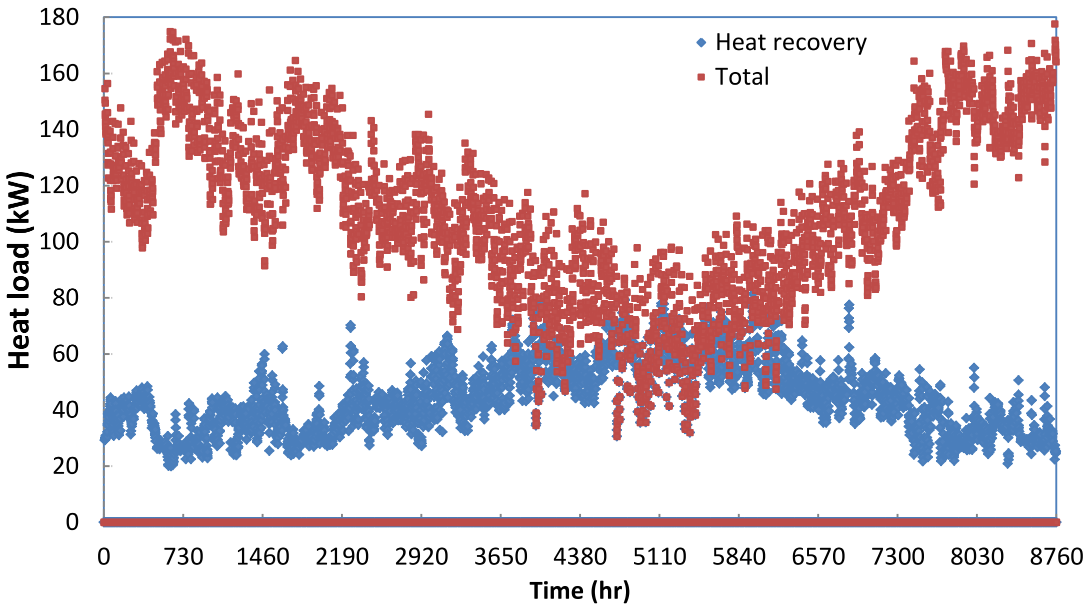

Fig. 11- Variations of space total heat load and heat recovery from refrigeration discharge for CO_2 refrigeration system in one year period.

Table 1- CO_2 and R404A compressor specifications and the coefficients c_1~c_6 in the model

Ref.	Type	No.	Cycle	Q_{ev}/W_{cp}	c_1	c_2	c_3	c_4	c_5	c_6
CO2	4FTC-20K	HT/10	Transcritical	W_{cp}	-9.334E-04	4.086E-01	-6.053E-03	-5.150E-01	6.033E-03	-7.402E+00
				Q_{ev}	-1.222E-03	3.368E+00	1.772E-02	-4.468E+00	-1.146E-02	-1.083E+01
	2EHC-3K	LT/5	Subcritical	W_{cp}	6.693E-04	2.205E-01	-2.050E-03	-1.336E-01	2.933E-03	2.086E+00
				Q_{ev}	-6.068E-04	-4.320E-01	8.146E-03	1.170E+00	-5.665E-03	4.270E+01
R404A	6J-22.2Y	HT/5	Subcritical	W_{cp}	-1.035E-03	4.161E-01	-1.672E-03	-3.490E-02	9.045E-03	9.689E+00
				Q_{ev}	6.466E-04	-1.142E+00	2.505E-02	3.513E+00	-2.284E-02	1.208E+02
	6J-22.2Y	LT/5	Subcritical	W_{cp}	-1.035E-03	4.161E-01	-1.672E-03	-3.490E-02	9.045E-03	9.689E+00
				Q_{ev}	6.466E-04	-1.142E+00	2.505E-02	3.513E+00	-2.284E-02	1.208E+02

Table 2- Control parameters for CO_2 and R404A refrigeration systems

Location	System	High side pressure control				Suction pressure control	
			Supercritical	**Subcritical**		**Tsuct,sat(°C)**	
		TT (°C)	**Optimal pressure control**	**Floating pressure control**		**MT pack**	**LT pack**
				Tcond_min (°C)	**DT (K)**		
Glasgow	**R404A Multiplex**	**N/A**	**N/A**	**20 for MT ; 10 for LT**	**15 for MT ; 10 for LT**	**-10**	**-32**
	CO_2 Booster	**21**	**Yes**	**10**	**10**	**-10**	**-32**

Table 3- Electrical energy consumption and space heating thermal energy during a year

System	Wcomp (kWh)				Wfan (kWh)				Total (kWh)	Qvent (kWh)		
	MT/HT	LT-1	LT-2	Total	HT/MT	LT-1	LT-2	Total		Total	Heat recovery	Saving(%)
R404A	409575	91302	100322	601198	62625	15654	17131	95409	696607	420115	0	0
CO2	536243	81071		617315		95584		95584	712899	420654	168399	40